MRS Communications (2019), *9*, 1087–1092
© The Author(s) 2019
doi:10.1557/mrc.2019.97

MRS Communications

Research Letter

Morphological effects on the third-order nonlinear optical response of polydiacetylene nanofibers

Haruki Maki, Rie Chiba, Tsunenobu Onodera, and **Hitoshi Kasai**, Institute of Multidisciplinary Research for Advanced Materials (IMRAM), Tohoku University, Katahira 2-1-1, Aoba-ku, Sendai 980-8755, Japan
Rodrigo Sato and **Yoshihiko Takeda**, Hydrogen Materials Engineering Group, Center for Green Research on Energy and Environmental Materials, National Institute for Materials Science (NIMS), Sakura 3-13, Tsukuba 305-0003, Japan
Hidetoshi Oikawa, Institute of Multidisciplinary Research for Advanced Materials (IMRAM), Tohoku University, Katahira 2-1-1, Aoba-ku, Sendai 980-8755, Japan

Address all correspondence to Hidetoshi Oikawa at **hidetoshi.oikawa.e8@tohoku.ac.jp**

(Received 16 May 2019; accepted 8 July 2019)

Abstract

The third-order nonlinear optical (NLO) susceptibility for morphologically controlled polydiacetylene (PDA) nanocrystals (NCs) and PDA nanofibers (NFs) have been determined for the first time by the experimental combination of transient pump-probe spectroscopy and spectroscopic ellipsometry. The figure of the merit of PDA NFs was much superior to PDA NCs and/or PDA bulk crystals, and the excitonic relaxation time was of order of sub-pico second. Namely, this is the first case to reveal the morphological effect on NLO response. PDA NFs having the long effective π-conjugation length are one of the most promising organic third-order NLO nanomaterials toward the photonic device application.

Introduction

A nonlinear optical (NLO) response is one of the most important optical process and key technology toward next-generation optoelectronic and/or photonic device applications,[1] e.g., optical wiring,[2] optical transistor,[3] random lasing,[4] optical memory,[5] and all optical computing system.[6] NLO materials should be needed to provide much large third-order NLO susceptibility, $\chi^{(3)}(\omega)$, and femto-second order of highly optical response so as to fulfill these optical and/or photonic devices. In common, organic NLO materials exhibit rapid optical response, whereas inorganic NLO materials take large $\chi^{(3)}(\omega)$.[7,8] Polydiacetylene (PDA) is synthesized by topochemical solid-state polymerization of diacetylene (DA) monomer in a crystal state and a unique one-dimensional π-conjugated polymer.[9] Some PDA derivatives are well known as one of the most promising organic NLO materials.[10,11]

Instead of material designs and synthetic developments, morphologically controlled nanostructures such as nanocrystallization and/or hybridization on a nano-scale level would be expected to further enhance NLO properties,[12] but this is still much challenging and interesting topics in current organic NLO material science, although the enhancement of $\chi^{(3)}(\omega)$ has been already reported in semiconductor quantum dots, owing to the quantum confinement effect.[12] On the other hand, π-conjugated organic and polymer nanocrystals (NCs) (hereinafter, organic NCs),[13,14] for example, PDA NCs and fluorescent perylene NCs, exhibited the dependence of linear optical properties, i.e., absorption and emission spectra, on crystal size, which is in the range of several tens nanometers to submicrometers. This is due to thermally softened crystal lattice structure with decreasing crystal size.[12–14] In other words, intermolecular optical interaction and/or strongly coupled exciton–lattice interaction in a short range should be reduced intensively with an increasing much large specific surface area in organic NCs.[15,16] It is, however, still unclear whether or not morphological effect like crystal size and shape would affect definitely the third-order NLO response from the viewpoint of enhancement of $\chi^{(3)}(\omega)$ in organic NLO nanomaterials.[17]

In the present article, PDA nanofibers (NFs) have been paid much an attention, and then the wavelength dispersions of $\chi^{(3)}(\omega)$ for well-defined PDA NCs and PDA NFs have been evaluated with a high precision by suitably combining pump-probe spectroscopy and spectroscopic ellipsometry.[18–21] This would lead to the possibility to control and tune the third-order NLO properties through the morphological effect in organic NLO nanomaterials.

Materials and methods

Materials

1,6-di(*N*-carbazolyl)-2,4-hexadiyne (DCHD) was used as a DA monomer. DCHD, sodium dodecyl sulfate (SDS), and polyvinyl alcohol (PVA; degree of polymerization = 3100 and degree of saponification = above 96%) were purchased from Wako Pure Chemical Industries Ltd., Sendai, Japan and Sigma-Aldrich Co. LLC, Sendai, Japan, respectively. The solvents with 99%

https://doi.org/10.1557/mrc.2019.97 Published online by Cambridge University Press

purity or greater were all purchased from Wako Pure Chemical Industries Ltd. and used without purification.

Fabrications of PDA NCs, PDA NFs, and PDA bulk crystals, and their characterization

PDA NCs were prepared by the conventional reprecipitation method,[13,14] and PDA NFs were also fabricated as follows.[17] A 200 μL of DCHD–acetone solutions (5 mM) containing SDS (1 mM) was quickly injected into vigorously stirred pure water (10 mL) as a poor medium at given temperature, after the retention time for about 30 min, followed by UV irradiation (λ = 254 nm, 1.55 W/m^2) to convert DA into the corresponding PDA [poly(DCHD)] through solid-state polymerization.[9] The resulting PDA NCs and PDA NFs were characterized with a scanning electron microscope (SEM; JEOL, JSM-6700F) after the platinum sputtering process and with a UV–Vis absorption spectrophotometer (JASCO, V-570). On the other hand, DCHD was crystallized by slow-evaporating saturated DCHD–DMF solutions at 5 °C for a few months. The obtained DCHD bulk crystals were further irradiated with γ-ray irradiation from ^{60}Co radiation source so as to prepare PDA [poly(DCHD)] bulk crystals. Powder x-ray diffraction (XRD) patterns for PDA NCs, PDA NFs, and PDA bulk crystal were measured with x-ray diffractometer (Bruker, D8 ADVANCE, Cu K$_\alpha$: 0.154 nm) (Supplementary Fig. S1). The crystal dimensions of the resulting PDA bulk crystal are about 5 mm (length) × 3 mm (width) × 1 mm (height) in crystal size without having macroscopically voids and cracks from the photograph [Inset in Supplementary Fig. S1(d)].

PVA composite thin films of PDA NCs and/or PDA NFs

PVA composite thin films of PDA NCs and/or PDA NFs with highly optical quality were fabricated as follows. An aqueous dispersion liquid (1.0 mL) of PDA NCs (or PDA NFs) was mixed with PVA aqueous solution (0.14 wt%, 0.1 mL) and then water medium was evaporated rapidly on an quartz substrate (KU1) heated around at 100 °C.

Measurements of transient transmission spectrum and complex refractive index for evaluating NLO properties

As given by Eqs. (1) and (2), the wavelength dispersions of $\chi^{(3)}(\omega)$ have been evaluated from the variations of complex dielectric function, $\Delta\varepsilon^*(\omega) = \Delta\varepsilon'(\omega) + i\cdot\Delta\varepsilon''(\omega)$, by means of the experimental combination of transient response with femtosecond (fs) pump-probe spectroscopy (Supplementary Fig. S2) and optical analysis with spectroscopic ellipsometry.[18–21]

$$\Delta\varepsilon'(\omega) = \frac{3}{4}\mathrm{Re}[\chi^{(3)}(\omega)]|E|^2 \quad (1)$$

$$\Delta\varepsilon''(\omega) = \frac{3}{4}\mathrm{Im}[\chi^{(3)}(\omega)]|E|^2 \quad (2)$$

where $|E|^2$ is the intensity of incident laser light, and 3/4 means K-factor for the intensity-dependent refractive index.

Transient transmission spectrum, $\{\Delta T(\omega) + T(\omega)\}/T(\omega)$, was measured with the pump-probe method having a fs-pulsed Ti: sapphire laser system (Spectra-Physics, Inc., Mai-tai and Spitfire) with BBO (β-BaB_2O_4) crystal for second harmonic generation (Supplementary Figs. S2 and S3). As a pump beam, the incident laser pulse (λ = 400 nm, 150 fs, 0.5 kHz) was irradiated to PVA composite thin films through the optical delay system, and the probe beam was continuum white light (1.0 kHz) through a self-phase modulator of sapphire. On the other hand, linear complex dielectric function, $\varepsilon^*(\omega) = \varepsilon'(\omega) + i\cdot\varepsilon''(\omega)$, and film thickness were evaluated by the use of a variable angle spectroscopic ellipsometer (J. A. Woollam Co., Inc., M-1000 and CompleteEASE) with multiple angles of incidence with steps of 10° from 50° to 80° in the wavelength range from 200 to 1000 nm (Supplementary Fig. S4). The wavelength dispersion of $\varepsilon^*(\omega)$ was obtained by using some oscillator models (Lorentz and interband contribution model and Cauchy function model) under the assumption of homogeneously suitable optical models. $T(\omega)$ is simulated from the analyzed dispersion, and then the measured $\{\Delta T(\omega) + T(\omega)\}/T(\omega)$ is multiplied by $T(\omega)$ to calculate the modulated component, $\Delta T(\omega) + T(\omega)$. The small modulation can derive $\varepsilon'(\omega) + \Delta\varepsilon'(\omega)$ and $\varepsilon''(\omega) + \Delta\varepsilon''(\omega)$ in the ellipsometric analysis according to causality of Kramers–Kronig. Finally, one can estimate $\Delta\varepsilon'(\omega)$ and $\Delta\varepsilon''(\omega)$ at the left sides in Eqs. (1) and (2) so as to determine $\chi^{(3)}(-\omega_{\mathrm{probe}}; \omega_{\mathrm{probe}}, -\omega_{\mathrm{pump}}, \omega_{\mathrm{pump}})$ in the present case. There is the corresponding absorption to the extinction coefficient at the pumping wavelength (λ = 400 nm) as shown in Supplementary Fig. S4. In addition, the measurements have been performed with the polarized pump beams in parallel with the b-axis (π-conjugation) direction of the bc-plane in the case of PDA bulk crystal.[22]

Results and discussion

Figure 1 shows the SEM images of PDA NCs and PDA NFs. It is possible to control the diameter and counter length of PDA NFs by changing water temperature as a poor medium in the reprecipitation method.[17] The diameter of PDA NFs was about 50 nm, and the counter length was above a few μm. The conversion of solid-state polymerization is 100% in the present case, owing to characteristic mechanism of monomer crystal-to-polymer crystal-phase transition.[13,14,17] In addition, PDA NFs have the same crystal lattice structure as PDA NCs and/or PDA bulk crystals (Supplementary Fig. S1).[17]

PDA has the excitonic absorption peak around at λ = 650 nm, which is originated from π-conjugation along the PDA backbone formed by solid-state polymerization, and broad phonon-side band around at λ = 580–620 nm.[9] Figure 2 indicates the extinction (excitonic absorption) spectra of PDA NCs and PDA NFs. In PDA NFs, the excitonic absorption peak was clearly stronger than the small intensity of phonon-side band, which tendency is basically similar to PDA bulk crystals. On the other hand, the extinction of excitonic absorption peak

https://doi.org/10.1557/mrc.2019.97 Published online by Cambridge University Press

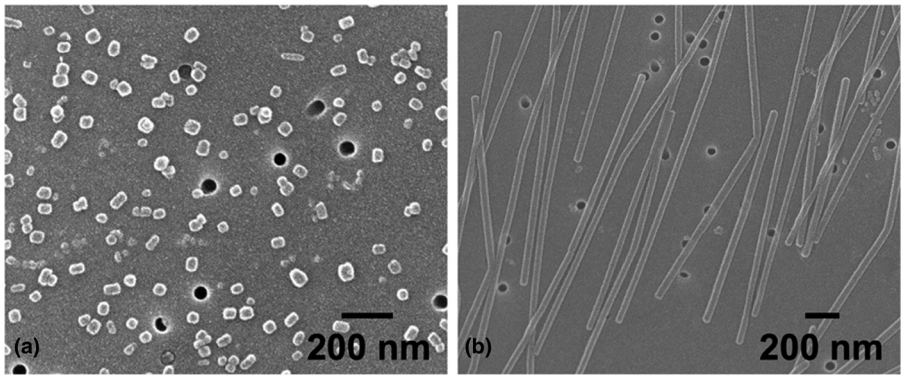


Figure 1. SEM images of (a) PDA NCs and (b) PDA NFs.

(excitonic absorbance) is inclined to diminish with decreasing crystal size.[12–14] Interestingly, the excitonic absorption peak position of PDA NFs ($\lambda_{exc,\ PDA\ NFs} = 659$ nm) was so red-shifted, rather than typical PDA NCs with approximately 50 nm in crystal size ($\lambda_{exc,\ PDA\ NCs} = 633$ nm) and/or PDA bulk crystal ($\lambda_{exc,\ PDA\ bluk\ crystal} = 655$ nm). These facts suggest that the effective π-conjugation length along the PDA backbone became much longer in PDA NFs, compared with PDA NCs and/or PDA bulk crystals, and then the enhancement of $\chi^{(3)}(\omega)$ is expected according to the theoretical prediction by so-called the three-state model.[20] On the other hand, the *bc*-plane surface of PDA bulk crystal has a luster like a facet shown in the inset in Supplementary Fig. S1(d), and the optical quality was confirmed to be enough suitable from the measurements with pump-probe spectroscopy [Supplementary Fig. S3(b)] and spectroscopic ellipsometry [Supplementary Fig. S4(c)].

Figure 3 exhibits the wavelength dispersions in the real and imaginary parts of effective $\chi^{(3)}(\omega)$, $\chi^{(3)}_{eff}(\omega)$, in both cases of PDA NCs and PDA NFs, which were evaluated from the transient transmission spectrum (Supplementary Fig. S3) and complex refractive index, $n^*(\omega) = n(\omega) + i \cdot k(\omega) = \varepsilon^*(\omega)^{1/2}$,

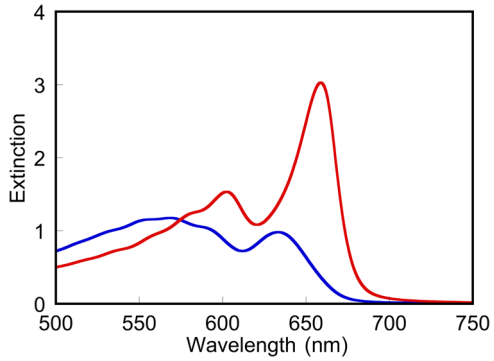


Figure 2. Extinction (excitonic absorption) spectra for aqueous dispersion liquids of PDA NCs (blue sold line: $\lambda_{exc,\ PDA\ NCs} = 633$ nm, ~50 nm in crystal size) and of PDA NFs (red solid line: $\lambda_{exc,\ PDA\ NFs} = 659$ nm). PDA bulk crystals exhibit $\lambda_{exc,\ PDA\ bulk\ crystal} = 655$ nm.

(Supplementary Fig. S4) as described in Materials and Methods. The obtained $\chi^{(3)}_{eff}(\omega)$ means the optical constant of $\chi^{(3)}(\omega)$ for the whole thin films of PVA composites that contained PDA NCs and/or PDA NFs. From the overviews in Fig. 3, the intensity of $\chi^{(3)}_{eff}(\omega)$ in PDA NFs was obviously larger than that of PDA NCs in the broad wavelength range including the excitonic absorption region, i.e., in both resonant and non-resonant regimes. In addition, the present NLO response time (the excitonic relaxation time) was typically 0.65 ps in the case of PDA NFs (Supplementary Fig. S5), which suggests an ultra-fast optical response without the thermal relaxation process even in the resonant region.[23] To our knowledge, the present experimental results are the first example that could clearly reveal the morphological effect on (or difference in) $\chi^{(3)}(\omega)$ in organic NLO nanomaterials, except for the enhancement of $\chi^{(3)}(\omega)$ by the quantum confinement effect in semiconductor quantum dots.[24,25]

In general, the wavelength dispersions of $\chi^{(3)}_{eff}(\omega)$ would be a reflection of the extinction spectra as shown in Fig. 2. Especially, the minimum of $\mathrm{Im}[\chi^{(3)}_{eff}(\omega)]$ corresponds to the excitonic absorption peak, while $\mathrm{Re}[\chi^{(3)}_{eff}(\omega)]$ behaviors are closely correlated with the refractive index that is in common changed sharply at the lower energy region in the vicinity of the excitonic absorption peak position.[26] Actually, the obtained $\chi^{(3)}_{eff}(\omega)$ is affected by some experimental factors in PVA composite thin films, that is, thickness, optical absorption and scattering loss, and volume fraction of PDA NCs and/or PDA NFs. The figure of merit (FOM) is often introduced to avoid above-mentioned effects and/or problems and usually defined as the absolute value of $\chi^{(3)}_{eff}(\omega)$ normalized reasonably and properly by a factor such as absorbance, $A_{Abs}(\omega)$: $\mathrm{FOM} = |\chi^{(3)}_{eff}(\omega)|/A_{Abs}(\omega)$.[27] $A_{Abs}(\omega)$ is experimentally calculated from the measured extinction, $A_{Obs}(\omega)$, under the semi-empirical assumption of the following additive property: $A_{Obs}(\omega) = A_{Abs}(\omega) + A_{Scat}(\omega)$, where $A_{Scat}(\omega)$ is a scattering factor and given by $C \cdot \omega^n$ (C: constant and n: adjustable exponent) on the basis of generalized Rayleigh scattering theory.[28] FOM, however, would diverge at nonresonant regime in the present case because of substantially $A_{Obs}(\omega) \approx A_{Abs}(\omega) \approx A_{Scat}(\omega) \approx 0$ at

https://doi.org/10.1557/mrc.2019.97 Published online by Cambridge University Press

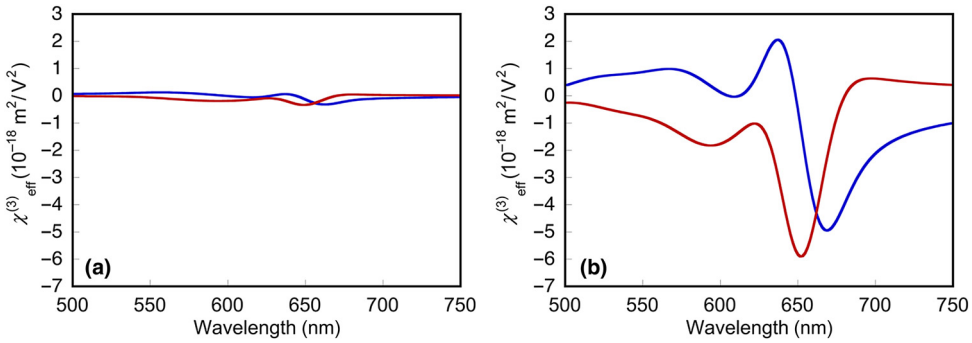


Figure 3. Wavelength dispersions of effective $\chi^{(3)}(\omega)$, $\chi^{(3)}_{\text{eff}}(\omega)$: (a) PDA NCs at $E = 2.27 \times 10^8$ V/m and (b) PDA NFs at $E = 1.88 \times 10^8$ V/m, where E is the electric field strength of the pump beam. Blue and red solid lines are the real and imaginary parts of $\chi^{(3)}_{\text{eff}}(\omega)$, respectively.

the long wavelength region as shown in Fig. 2. So, FOM was redefined as $\text{FOM} = |\chi^{(3)}_{\text{eff}}(\omega)|/|\chi^{(1)}(\omega)|$ without using $A_{\text{Abs}}(\omega)$, where $\chi^{(1)}(\omega)$ is the first-order linear optical susceptibility and given by $\varepsilon^*(\omega) = 1 + \chi^{(1)}(\omega)$. As a result, $\text{FOM}_{\text{PDA NFs}}$ is 2.24×10^{-18} m^2/V^2 in PDA NFs, whereas $\text{FOM}_{\text{PDA NCs}}$ is 5.65×10^{-19} m^2/V^2 in PDA NCs. Therefore, $\text{FOM}_{\text{PDA NFs}}$ is higher than $\text{FOM}_{\text{PDA NCs}}$ by a factor of about 4, closely relating that the effective π-conjugation length of the PDA backbone is relatively much longer in PDA NFs as discussed in Fig. 2.

Next, the intrinsic values of $\chi^{(3)}_{\text{eff, Single PDA NF}}(\omega)$ and $\text{FOM}_{\text{Single PDA NF}}$ for the single component of PDA NF were compared with those of PDA bulk crystal as shown in Fig. 4. The volume fraction of PDA NFs, $f_{\text{PDA NFs}}$, was first calculated to be 0.028 in PVA composite thin films on the assumption of homogeneously nonaggregated loading of PDA NFs into the PVA matrix by employing the density of materials, d, as follows: $d_{\text{PDA NFs}} = 1.3$ g/cm^3 and $d_{\text{PVA}} = 1.27$ g/cm^3. The wavelength dispersion of $\chi^{(3)}_{\text{eff, Single PDA NF}}(\omega)$ could be calculated successfully by utilizing so-called the effective medium approximation model.[29] It has become apparent that the $\chi^{(3)}_{\text{Single PDA NF}}(\omega)$ was multiplied about one order of magnitude, by comparison with $\chi^{(3)}_{\text{PDA bulk crystal}}(\omega)$. Namely, $\text{FOM}_{\text{Single PDA NF}}$ is 1.07×10^{-17} m^2/V^2 and about 1.5 times superior to $\text{FOM}_{\text{PDA bulk crystal}} = 7.25 \times 10^{-18}$ m^2/V^2.

Let us further consider again about the dependences of the determined $\chi^{(3)}_{\text{eff}}(\omega)$ and FOM on crystal direction, orientation effect, and effective π-conjugation length, although those have already discussed somewhat in Figs. 2 and 3. The first point is the crystal direction, which is an important factor, when linear optical properties and the NLO response are discussed.[15–17] The direction of π-conjugation along the present PDA backbone is parallel to the long-axis direction of PDA NFs.[13,14] On the other hand, the *b*-axis corresponds to the direction of π-conjugation along the PDA backbone in a bulk crystal state.[22] In practice, PVA composite thin films were prepared as described in Materials and Methods. That is, the *a*-, *b*-, and *c*-axis directions are isotropically random in the films of PDA NCs, and the long-axis (and π-conjugation) direction of PDA NFs is parallel to a substrate surface and random in-plane of the films. On the other hand, the *bc*-plane of PDA bulk crystal is located in parallel on a substrate surface on the basis of the above-mentioned crystal dimension in Materials and Methods, and powder XRD data are displayed in Supplementary Fig. S1. Thus, these preparation conditions suggest that there is no influence of orientation effect in the present study when the resulting order (or superiority) of the magnitude of $\chi^{(3)}_{\text{eff}}(\omega)$ and/or FOM is compared among three kinds of PDA NCs, PDA NFs, and PDA bulk crystal, owing to the difference enough in $\chi^{(3)}_{\text{eff}}(\omega)$ and/or FOM as shown in Figs. 3 and 4.

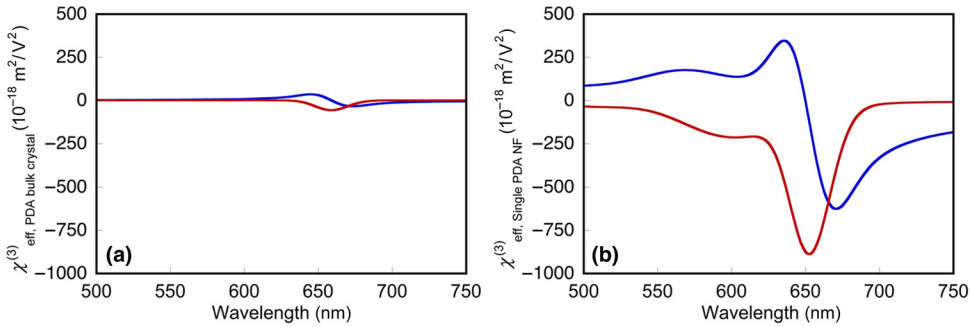


Figure 4. Wavelength dispersion of $\chi^{(3)}_{\text{eff}}(\omega)$: (a) PDA bulk crystal at $E = 1.74 \times 10^8$ V/m and (b) single PDA NF at $E = 1.57 \times 10^8$ V/m. Blue and red solid lines indicate the same symbols as in Fig. 3.

https://doi.org/10.1557/mrc.2019.97 Published online by Cambridge University Press

The second point is effective π-conjugation length.[30,31] The measured $\chi^{(3)}_{eff}(\omega)$ is extensively affected by band structure,[20] especially effective π-conjugation length along the polymer backbone (or the diffusion length of exciton), which is closely related to the distribution of the degree of polymerization[30,31], local steric hindrance, the conformational change of π-conjugated polymers, crystal defects, and so on.[7,9–17,22] For example, the excitonic absorption peak in PDA NCs is commonly blue-shifted with decreasing crystal size from a bulk crystal state.[12–14] This is the typical size effect of linear optical properties in organic NCs, and the effective π-conjugation length becomes shorter with decreasing crystal size, due to thermally soften crystal lattice (or reduction of intermolecular interaction in a crystal state) induced by the increase in a specific surface area.[15,16] Usually, mechanical strain is accumulated in the PDA backbone inside crystal lattice because of the difference in crystal cell parameters before and after solid-state polymerization.[7,15,16,22] Probably, mechanically accumulated strain could release smoothly in PDA NFs, since the rigidity of crystal lattice in PDA NFs is an intermediate state between PDA NCs and the corresponding bulk crystal.[17] Actually, the excitonic absorption peak in PDA NFs was more red-shifted than that in bulk crystal as shown in Fig. 2, which suggests that the PDA backbone is almost strain-free, less local steric hindrance, and then the longest effective π-conjugation length among the present three kinds of PDA samples.[13,14,16] On the other hand, it is often difficult to prepare defect-free organic and/or conjugated polymer bulk crystal, in which effective π-conjugation length along the polymer backbone does not necessarily correspond to the crystal dimensions.[12–14]

Namely, $\chi^{(3)}_{eff}(\omega)$ is, in principle, enhanced by the effectively long π-conjugation length and/or narrow band gap in the three-state model,[20] being strongly dependent on crystal morphology such as PDA NFs and/or PDA NCs.

Conclusions

It was obviously found that $\chi^{(3)}_{eff}(\omega)$ and FOM of PDA NFs were much higher than those of PDA NCs and/or the corresponding PDA bulk crystals because of sufficiently developed and grown effective π-conjugation of PDA backbone in PDA NFs. In addition, PDA NFs exhibited sub-pico second order of NLO response. These facts are exactly morphological effect on third-order NLO properties and would provide advantage in organic NLO nanomaterials. That is to say, one can expect more enhancement of $\chi^{(3)}_{eff}(\omega)$ and FOM for oriented thin films of PDA NFs[17] and/or for hybridization with plasmonic metal nanoparticles toward photonic device application.[32]

Supplementary materials

The supplementary material for this article can be found at https://doi.org/10.1557/mrc.2019.97.

Acknowledgment

The present research was performed under the Cooperative Research Program of "Network Joint Research Center for Materials and Devices" and "NIMS Joint Research Hub Program."

References

1. Z. Rinkevicius, X. Li, J.A.R. Sandberg, and H. Agren: Non-linear optical properties of molecules in heterogeneous environments: a quadratic density functional/molecular mechanics response theory. *Phys. Chem. Chem. Phys.* **16**, 8981 (2014).
2. M. Aljada, K.E. Alameh, Y.-T. Lee, and I.I.-S. Chung: High-speed (2.5 Gbps) reconfigurable inter-chip optical interconnects using opto-VLSI processors. *Opt. Exp.* **14**, 6823 (2006).
3. J. Hwang, M. Pototschnig, R. Lettow, G. Zumofen, A. Renn, S. Gotzinger, and V. Sandoghdar: A single-molecule optical transistor. *Nature* **460**, 76 (2009).
4. F. Luan, B. Gu, A.S.L. Gomes, K.T. Yong, S.C. Wen, and P.N. Prasad: Lasing in nanocomposite random media. *Nano Today* **10**, 168 (2015).
5. R. Okamoto, J.L. O'Brien, H.F. Hofmann, T. Nagata, K. Sasaki, and S. Takeuchi: An entanglement filter. *Science* **323**, 483 (2009).
6. S.D. Smith: Laser, nonlinear optics and optical computers. *Nature* **316**, 319 (1985).
7. H. Oikawa, T. Onodera, A. Masuhara, H. Kasai, and H. Nakanishi: New class materials of organic-inorganic hybridized nanocrystals/nanoparticles, and their assembled micro- and nano-structure toward photonics. *Adv. Polym. Sci.* **231**, 147 (2010).
8. O. Yarimaga, J. Jaworski, B. Yoon, and J.-M. Kim: Polydiacetylenes: supramolecular smart material with a structural hierarchy for sensing, imaging and display applications. *Chem. Commun.* **48**, 2469 (2012).
9. G. Wegner: Solid-state polymerization mechanisms. *Pure Appl. Chem.* **49**, 443 (1997).
10. H. Matsuda, S. Molyneux, A.K. Kar, B.S. Wherrett, S. Okada, and H. Nakanishi: Third-order nonlinear optical properties of polydiacetylene crystal. *J. Photopolym. Sci. Technol.* **6**, 261 (1993).
11. E. Giorgetti, G. Margheri, S. Sottini, X. Chen, A. Cravino, D. Comoretto, C. Cuniberti, C. Dell'Erba, and G. Dellepiane: Linear and nonlinear characterization of polyDCHD-HS films. *Synth. Met.* **115**, 257 (2000).
12. H. Oikawa: Hybridized organic nanocrystyals for optically functional materials. *Bull. Chem. Soc. Jpn.* **84**, 233 (2011).
13. H. Oikawa, H. Kasai, and H. Nakanishi: Fabrication of organic microcrystals and their optical properties. In *Anisotropic Organic Materials—Approaches to Polar Order, ACS Symposium Series 798*, edited by R. Glaser, and P. Kaszynski (ACS, Washington, 2001), pp. 158–168.
14. H. Oikawa and H. Nakanishi: Reprecipitation method for organic nanocrystals. In *Nano Science and Technology—Single Organic Nanoparticles*, edited by H. Masuhara, H. Nakanishi and K. Sasaki (Springer, Berlin, 2003), pp. 17–31.
15. H. Oikawa, T. Mitsui, T. Onodera, H. Kasai, H. Nakanishi, and T. Sekiguchi: Crystal size dependence of fluorescence spectra from Perylene nanocrystals evaluated by scanning near-field optical microscopy. *Jpn. J. Appl. Phys.* **42**, L111 (2003).
16. V.V. Volkov, T. Asahi, H. Masuhara, A. Masuhara, H. Kasai, H. Oikawa, and H. Nakanishi: Size-dependent optical properties of polydiacetylene nanocrystals. *J. Phys. Chem. B* **108**, 7674 (2004).
17. Y. Iimori, T. Onodera, H. Kasai, M. Mitsuishi, T. Miyashita, and H. Oikawa: Fabrication of pseudo single crystalline thin films composed of polydiacetylene nanofibers and their optical properties. *Opt. Mater. Exp.* **7**, 2218 (2017).
18. R. Sato, H. Momida, M. Ohnuma, M. Sasase, T. Ohno, N. Kishimoto, and Y. Takeda: Experimental dispersion of the third order optical susceptibility of Ag nanoparticles. *J. Opt. Soc. Am. B* **29**, 2410 (2012).
19. R. Sato, M. Ohnuma, K. Oyoshi, and Y. Takeda: Experimental investigation of nonlinear optical properties of Ag nanoparticles: effects of size quantization. *Phys. Rev. B* **90**, 125417 (2014).
20. R. Sato, M. Ohnuma, K. Oyoshi, and Y. Takeda: Spectral investigation of nonlinear local field effects in Ag nanoparticles. *J. Appl. Phys.* **117**, 113101 (2015).

https://doi.org/10.1557/mrc.2019.97 Published online by Cambridge University Press

21. R. Sato, S. Ishii, T. Nagao, M. Naito, and Y. Takeda: Broadband plasmon resonance enhanced third-order optical nonlinearity in refractory titanium nitride nanostructures. *ACS Photonics* **5**, 3452 (2018).
22. V. Enkelmann: Structural aspects of the topochemical polymerization of diacetylene. *Adv. Polym. Sci.* **63**, 91 (1984).
23. G.P. Agrawal, C. Cojan, and C. Flytzanis: Nonlinear optical properties of one-dimensional semiconductors and conjugated polymers. *Phys. Rev. B* **17**, 776 (1978).
24. M. Nomura, N. Kumagai, S. Iwamoto, Y. Ota, and Y. Arakawa: Laser oscillation in a strongly coupled single-quantum-dot-nanocavity system. *Nat. Phys.* **6**, 279–283 (2010).
25. F. Flory, L. Escoubas, and G. Berginc: Optical properties of nanostructured materials. *J. Nanophotonics* **5**, 052502 (2011).
26. R.A. Ganeev, and T. Usmanov: Nonlinear-optical parameters of various media. *Quantum Electron.* **37**, 605 (2007).
27. A.G. Astill: Material figures of merit for non-linear optics. *Thin Solid Films* **204**, 1 (1991).
28. D.A.G. Bruggeman: Calculation of various physics constants in heterogeneous substrates. I. Dielectricity constants and conductivity of mixed bodies from isotropic substances. *Ann. Phys.* **24**, 636 (1935).
29. D.E. Aspnes: Optical-properties of thin-films. *Thin Solid Films* **89**, 249 (1982).
30. H. Murata, N. Takada, T. Tsutsui, S. Saito, T. Kurihara, and T. Kaino: Spectra of $\chi^{(3)}(-3\omega;\omega,\omega,\omega)$ in poly(2,5-thienylenevinylene) thin films with controlled conjugation lengths. *J. Appl. Phys.* **70**, 2915 (1991).
31. W. Schrof, S. Rozouvan, T. Hartmann, H. Möhwald, V. Belov, and E. Van Keuren: Nonlinear optical properties of novel low-bandgap polythiophenes. *J. Opt. Soc. Am. B* **15**, 889 (1998).
32. B. Gu, C. Zhao, A. Baev, K.-T. Yong, S. Wen, and P.N. Prasad: Molecular nonlinear optics: recent advances and applications. *Adv. Opt. Photonics* **8**, 328 (2016).

https://doi.org/10.1557/mrc.2019.97 Published online by Cambridge University Press